Injection of a Body into a Geodesic: Lessons Learnt from the LISA Pathfinder Case

Daniele Bortoluzzi[d], M Armano[a], H Audley[b], G Auger[c], J Baird[n], P Binetruy[c], M Born[b], D Bortoluzzi[d], N Brandt[e], A Bursi[t], M Caleno[f] , A Cavalleri[g], A Cesarini[g], J Conklin[u], M Cruise[h], K Danzmann[b], I Diepholz[b], R Dolesi[g], N Dunbar[i], L Ferraioli[j], V Ferroni[g], E Fitzsimons[e], M Freschi[a], J Gallegos[a], L Gambini[d], C Garcia Marirrodriga[f] , R Gerndt[e], LI Gesa[k], F Gibert[k], D Giardini[j], R Giusteri[g], C Grimani[l], I Harrison[m], G Heinzel[b], M Hewitson[b], D Hollington[n], M Hueller[g], J Huesler[f], H Inchauspe[c], O Jennrich[f], P Jetzer[o], B Johlander[f], N Karnesis[k], B Kaune[b], I Koeker[e], N Korsakova[b], C Killow[p], I Lloro[k], R Maarschalkerweerd[m], S Madden[f], D Mance[j], V Martin[k], F Martin-Porqueras[a], I Mateos[k], P McNamara[f], J Mendes[m], L Mendes[a], A Moroni[t], P Nellen[v], M Nofrarias[k], S Paczkowski[b], M Perreur-Lloyd[p], A Petiteau[c], P Pivato[g], E Plagnol[c], P Prat[c], U Ragnit[f], J Ramos-Castroq[r], J Reiche[b], J A Romera Perez[f], D Robertson[p], H Rozemeijer[f], G Russano[g], P Sarra[t], A Schleicher[e], J Slutsky[s], C F Sopuerta[k], T Sumner[n], D Texier[a], J Thorpe[s], C Trenkel[i], H B Tu[g], D Vetrugno[g], S Vitale[g], G Wanner[b], H Ward[p], S Waschke[n], P Wass[n], D Wealthy[j], S Wen[g], W Weber[g], A Wittchen[b], A Zambotti[d], C Zanoni[d], T Ziegler[e], P Zweifel[j]

Abstract

Launch lock and release mechanisms constitute a common space business, however, some science missions due to very challenging functional and performance requirements need the development and testing of dedicated systems. In the LISA Pathfinder mission, a gold-coated 2-kg test mass must be injected into a nearly pure geodesic trajectory with a minimal residual velocity with respect to the spacecraft. This task is performed by the Grabbing Positioning and Release Mechanism, which has been tested on-ground to provide the required qualification. In this paper, we describe the test method that analyzes the main contributions to the mechanism performance and focuses on the critical parameters affecting the residual test mass velocity at the injection into the geodesic trajectory. The test results are also presented and discussed.

d University of Trento, Trento, Italy
a European Space Astronomy Centre, European Space Agency, Madrid, Spain
b Albert-Einstein-Institut, Hannover, Germany
c Universite Paris Diderot, Paris, France
e Airbus Defence and Space, Immenstaad, Germany
f European Space Technology Centre, European Space Agency, Noordwijk, The Netherlands
g Dipartimento di Fisica, Universita di Trento, Trento, Italy
h Department of Physics and Astronomy, University of Birmingham, Birmingham, UK
i Airbus Defence and Space, Stevenage, UK
j Institut fur Geophysik, Zurich, Switzerland
k Institut de Ciencies de l'Espai, Bellaterra, Spain
l Istituto di Fisica, Universit_a degli Studi di Urbino, Urbino, Italy
m European Space Operations Centre, Darmstadt, Germany
n The Blackett Laboratory, Imperial College London, UK
o Physik Institut, Universitat Zurich, Zurich, Switzerland
p SUPA, Institute for Gravitational Research, University of Glasgow, Glasgow, UK
q Department d'Enginyeria Electronica, Universitat Politecnica de Catalunya, Barcelona, Spain
r Institut d'Estudis Espacials de Catalunya, Barcelona, Spain
s NASA Goddard Space Flight Center, Greenbelt, MD
t CGS S.p.A, Compagnia Generale per lo Spazio, Milano, Italy
u Department of Mechanical and Aerospace Engineering, University of Florida, Gainesville, FL
v RUAG Space, Zurich, Switzerland

Proceedings of the 43rd Aerospace Mechanisms Symposium, NASA Ames Research Center, May 4-6, 2016

Introduction

In LISA Pathfinder, some of the critical technologies developed for the in-space detection of gravitational waves will be tested [1] [2]. Scope of the mission is to set a 2-kg gold-coated AuPt test mass (TM) into a purely geodesic trajectory, i.e., bring it to free-fall condition inside the spacecraft by reducing any force other than gravity under the level of 10 $fN/Hz^{1/2}$ in the measurement bandwidth (1-30 mHz). Such a challenging requirement drove the design of the whole mission. In particular, the Gravitational Reference Sensor hosting the proof mass is internally gold coated and large gaps are present in order to limit the stray forces produced by local sources (i.e., charge patches). The Caging and Vent Mechanism secures the TM during the launch [3], while the Grabbing Positioning and Release Mechanism (GPRM) handles it in orbit and injects it into the geodesic trajectory (Figure 1) [4] [5].

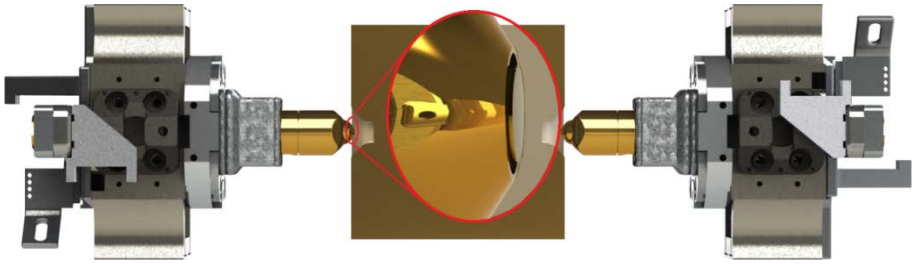

Figure 1. The Test Mass held by the two opposed GPRMs with detail of the release tip

We focus here on the latter phase performed by the GPRM, in which the TM is gently held in the center of the Gravitational Reference Sensor electrode housing by two opposed release-dedicated tips and then is left in free fall after their quick retraction. The critical requirement of this phase, determined by the capability of the capacitive control system to catch and re-center the TM after release, is the TM residual velocity, which must be below 5 μm/s. The nominal design of the two opposed GPRM release mechanisms provides a symmetric action on both sides of the TM, therefore perfect cancelation of forces and zero residual velocity. However, the ground testing of the release system highlighted some asymmetries. First, adhesive bonds are produced at both TM-release tip contacts [6], whose strength is affected by the surface topography at the microscopic scale, which is not controlled by the conventional machining processes. This converts into a low-repeatable adhesion behavior and high probability of non-cancelation of its effect on the two opposed TM sides (Figure 2 right). Second, some asymmetry is present also on the motion of the tips, which are commanded by two different actuators (for instance, if one of the tips is actuated with a time lag and/or moves with a different velocity, Figure 2 center). Even in the absence of adhesion this asymmetry makes the contact force time history different at the two opposed contacts, with a net contribution of their time integral, i.e., developed impulse. Referring to Figure 2 left, the net impulse is represented by the area enclosed by the two force-time histories, which quantifies the overall level of asymmetry of the two contacts.

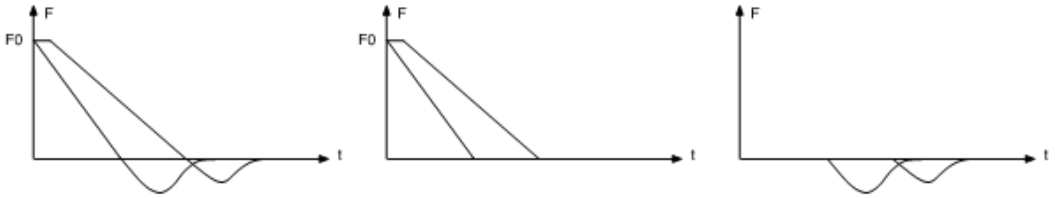

Figure 2. Asymmetry of contact forces on the TM (positive=pushing), pushing actions (preload) and pulling actions (adhesion)

The test approach is twofold. The effect of pushing forces (Figure 2 center) is ruled by the behavior of the mechanism (the holding force control level, the repeatability of the retraction) and is quantified by analysis

of the tests of retraction of the piezo and the holding force accuracy level. The effect of pulling forces (Figure 2 right) is ruled by the behavior of adhesion and is quantified by the tests performed with the Transferred Momentum Measurement Facility (TMMF, Figure 3) [7] [8] [9] [10] [11]. The in-flight environment is reproduced by suspending the TM mock up as a pendulum inside a vacuum chamber, and the release experiment consists in the approach and retraction of the tip with subsequent measurement of the swing oscillation produced (i.e., the transferred momentum) [12]. In order to maximize the representativeness of the experiment, in the latest test configuration of the TMMF the EQM of the GPRM is integrated to perform the release phase of the TM.

The two effects may be added since in flight there is no effect of the first effect to the second. This is motivated by the fact that the net velocity produced by the pushing actions (acting first) is negligible with respect to the velocity of retraction of the tip (about three orders of magnitude).

In-Flight Release Dynamics

Tests performed with the previous set-ups and contact mechanics models show that the tip-TM contact persists with relative displacements (from initial penetration under 0.3 N to final elongation at the detachments) of a few microns. By choosing a reference displacement value for the detachment (say 2 μm), it is possible to quantify the statistic distribution of the time required to obtain the separation of the tip from the TM. If we consider the tests performed by RUAG on the retraction quickness of the tip – unloaded – by restricting the results to the 24 tests performed on the flight models (FM1, FM2, FM3, FM4, nominal and redundant piezos [13]), we obtain a representative dispersion of the time to 2 μm as shown in Figure 4. The mean and standard deviation of the time to 2 μm are 0.04 ms and 0.005 ms respectively.

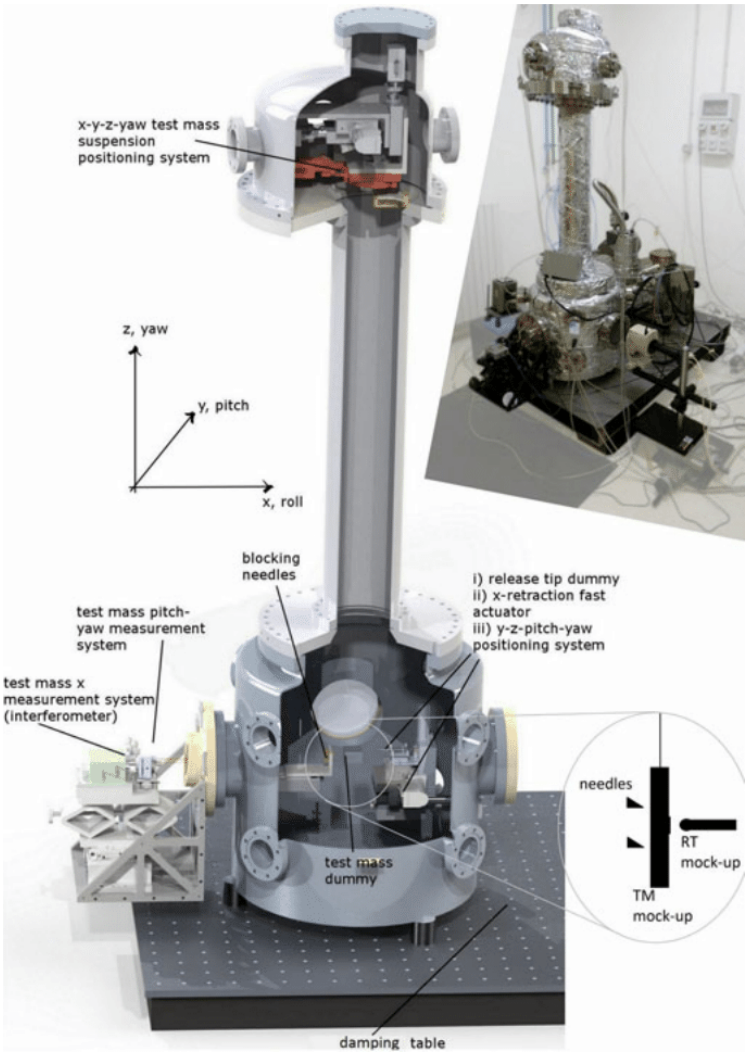

Figure 3. The Transferred Momentum Measurement Facility

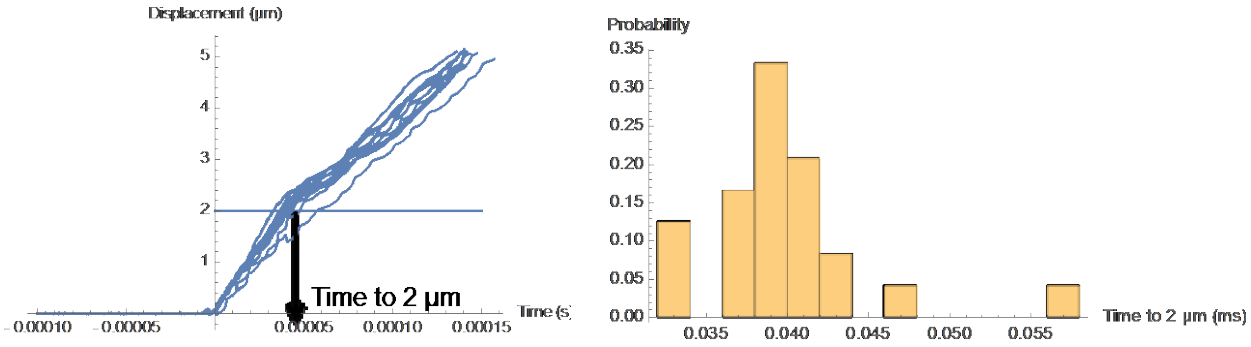

Figure 4. Time histories of the FM tip retraction (left) - Time to 2μm, statistical distribution (right)

Since the pushing force asymmetry is produced by the non-repeatability of the mechanism, we calculate the statistical distribution of the differences among times to 2 μm, which is shown in Figure 5. The standard deviation is about 7 μs.

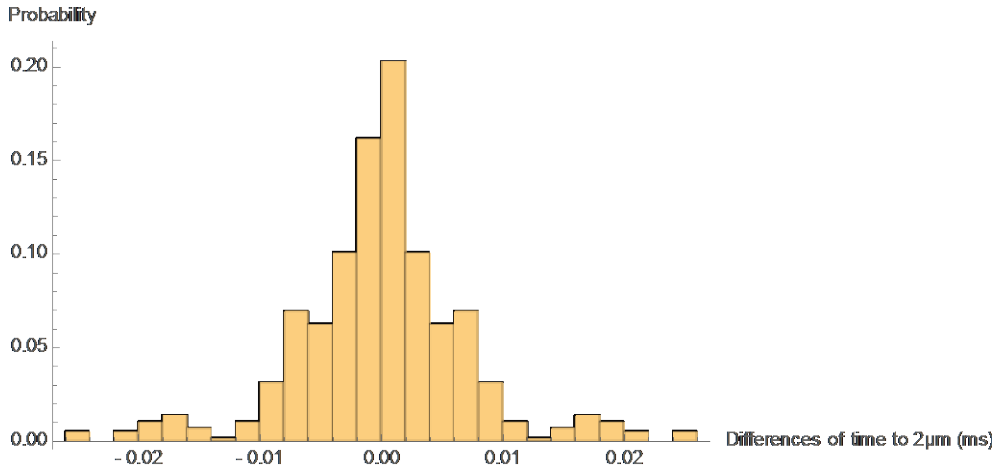

Figure 5. Statistical distribution of the differences of time to 2µm

Measurements performed at MAGNA show that the voltage drops 120 V – 0 V commanded by the Caging Control Unit to the two piezo stacks have a fair synchronization but are characterized by a different slope (in particular during the incipient motion), as shown in Figure 6.

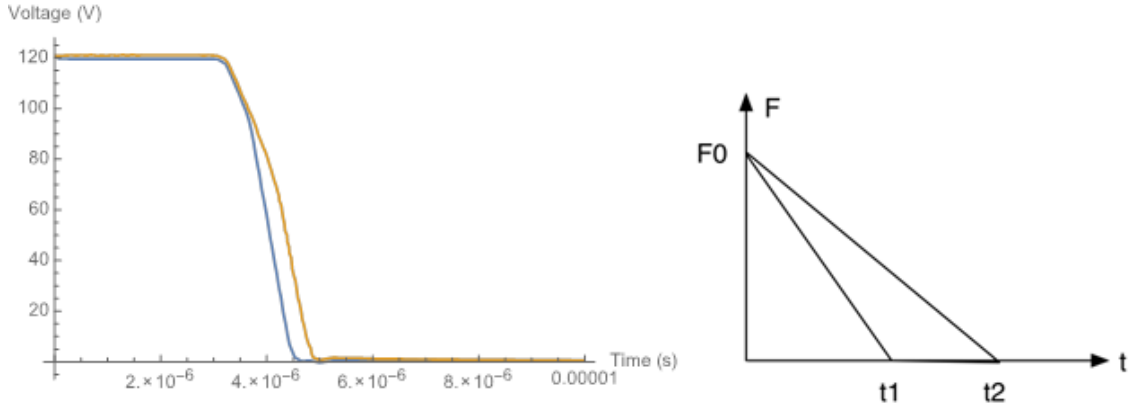

Figure 6. Caging Control Unit voltages commanded to the two stacks (left, courtesy of MAGNA) - Approximated resulting pushing force profiles (right)

As a consequence, the time lag between the two force time histories is assumed negligible and their behavior is assumed linear up to the zero level force (Figure 6 right). The net impulse given by such time histories is calculated and the TM velocity produced by the pushing forces can be calculated as follows:

$$v_{F0} = \frac{1}{2}\frac{F0}{m_{TM}}\Delta t \tag{1}$$

where *F0* is the initial holding force (about 0.3 N), m_{TM} is the flight TM mass and Δt is the difference between time *t2* and *t1* as in Figure 6 right. The resulting statistical distribution of the TM velocity produced by the pushing actions is plotted in Figure 7. The mean is zero (each difference is calculated also with inverted order of the two velocities), while the standard deviation is 0.5 µm/s.

Figure 7. Statistical distribution of the TM velocity produced by the pushing forces

If we add the contribution of adhesion to the effect of the pushing forces, the total in-flight velocity is given by the following formula:

$$v_{flight} = \frac{1}{2}\frac{F0}{m_{TM}}\Delta t + \frac{1}{m_{TM}}\Delta\left(\frac{\Delta U}{v_{RT}}\right) \quad (2)$$

where ΔU is the adhesion energy [14], v_{RT} is the velocity of the release tip at the detachment from the TM, $\Delta(\Delta U/ v_{RT})$ is the difference between the above quantities relative to the two contacts. The object of the TMMF ground testing is the quantification of the second term in Equation 2.

On-Ground Release Testing

The Transferred Momentum Measurement Facility

The past testing activities showed that adhesion occurring at the contacting surfaces produces a pull on the TM due to the retraction of the release-dedicated tip, up to bond failure. In the tests, care must be taken to minimize all environmental effects related to the laboratory, which may affect the adhesion dynamic failure and the developed pulling impulse. In the test set-up of the TMMF, the representativeness of the in-flight TM release conditions is based on the following:

- integration of the GPRM EQM -Z inside the vacuum chamber
- representative vacuum level (around 10^{-7} mbar)
- adoption of representative material of the TM bulk (Au-Pt alloy), machining process (Kugler) and gold coating (Selex Galileo)
- adoption of the same contact load (0.3 N).

The following differences between the test configuration and the flight configuration are present:

- mass of the TM mock-up. Based on the past test campaigns, the intermediate mass configuration (TM mock-up of 0.0883 kg) is chosen. With respect to the heavy (0.844 kg) and light (0.0096 kg) configuration, this allowed for a more detectable adhesion contribution
- cleanliness. The TM mock-up surface has been cleaned by means of isopropyl alcohol with ultra-sound bath. A mild baking procedure has been performed in vacuum to enhance outgassing. The whole experiment is located inside an ISO6 (class 1000) clean room
- one sided release. This configuration has been chosen since the early stages of the test activity. The main advantage consists in the absence of cancelation of the two opposed adhesion impulses, maximizing the sensitivity of the experiment to the release velocity
- gold-coated release tip. The GPRM EQM release tip is made of gold-coated TiAlV alloy.

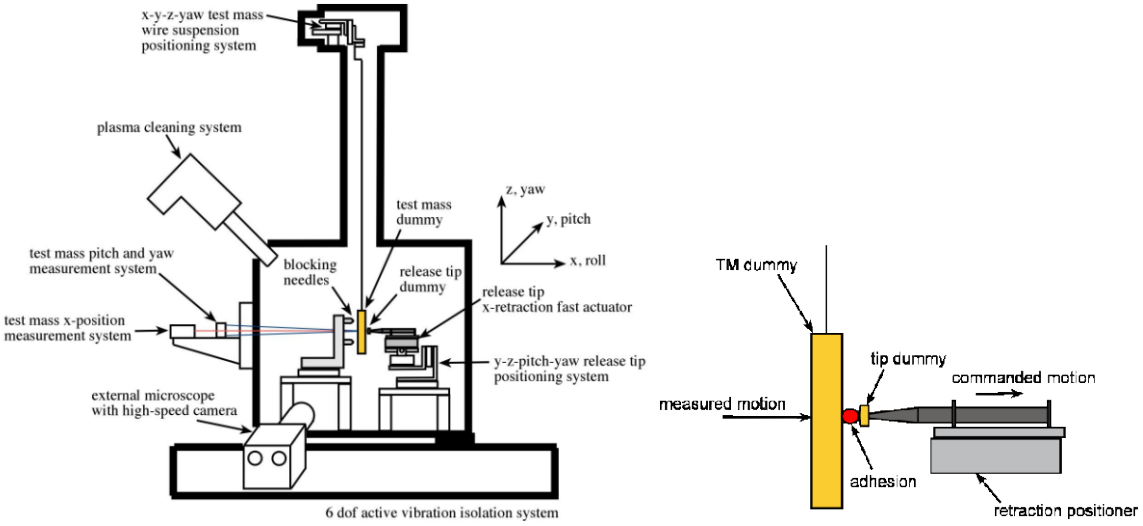

Figure 8. Old test configuration (before GPRM integration)

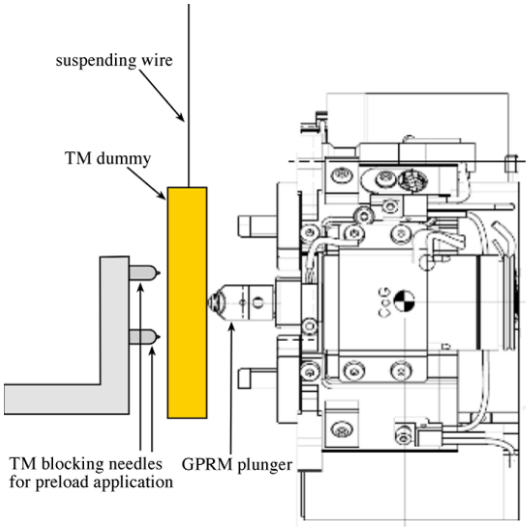

Figure 9. Test configuration with GPRM EQM –Z

In Figure 8 the TMMF configuration before the integration of the GPRM EQM is shown. In Figure 9 the test configuration with GPRM EQM is shown: the axis of retraction of the release tip is horizontal, engaging the TM mock-up in the center. The TM x displacement is measured by a laser interferometer, while the TM pitch and yaw angles are measured by a position sensing device through an optical lever system. The GPRM attitude (both pitch and yaw angles) can be adjusted to explore different directions of retraction of the tip. This is used both to search the maximum release velocity and to characterize its statistical distribution when the retraction is repeated with a representative misalignment of that occurring in flight. Pictures of TMMF and GPRM current setup are shown in Figure 10.

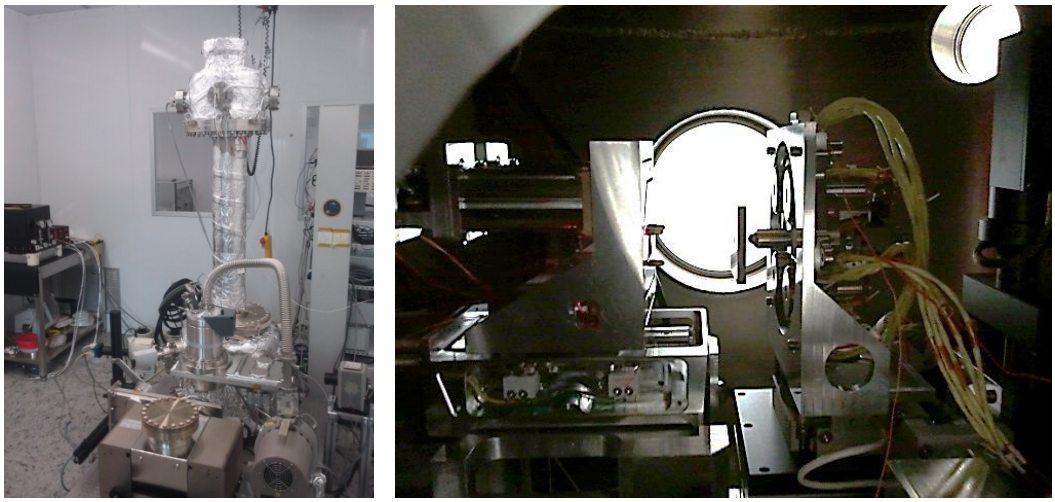

Figure 10. The TMMF in the clean room (left) – Blocking system, suspended TM and GPRM in the vacuum chamber (right)

On ground release dynamics

During the engagement, the TM mock-up is blocked on its rear side by three needles, which are actuated to adjust their attitude and allow engaging the TM with a minimal variation of its pitch and yaw angles with respect to the equilibrium. According to the tested GPRM handover procedure from the grabbing plunger to the release tip, the tip to TM contact force before the release is set to 0.3 N. This residual holding force is balanced by the blocking needles, which are not retracted during the release and produce an elastic push on the TM when the load is recovered at the retraction of the tip. As a consequence, the measured velocities are affected by this systematic contribution, which following the nominal in-flight procedure (nearly synchronous two-sided release) will be much smaller. The force-time histories plotted in Figure 2 left in the test configuration are modified as shown in Figure 11. The force applied by the release tip starts from *F0* and quickly drops to zero, exerts the adhesive pull and vanishes in a time frame of 0.04 ms, while the push of the blocking needles produce a cosine-like force profile which relaxes in a time frame of about 0.4 ms.

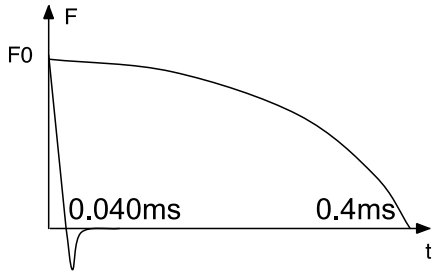

Figure 11. Force-time histories on the TM in the on-ground configuration

The stiffness of the blocking system is about $6 \cdot 10^5$ N/m, which is on the same order of magnitude of the axial stiffness of the GPRM. This means that the tested configuration is representative of an in-flight one-sided release. If the measured velocities are rescaled by the flight TM to mock-up ratio (about 20), they describe the TM velocity produced by a release performed by the retraction of just one tip. The TM velocity produced by the experiment can be calculated as follows:

$$v_{test} = \frac{F0}{\sqrt{m_{mockup} k_{needles}}} + \frac{1}{m_{mockup}} \frac{\Delta U}{v_{RT}} \tag{3}$$

where m_{mockup} is the mass of the TM mock-up and $k_{needles}$ is the stiffness of the blocking needles. The control uncertainty of the force *F0* is not negligible and the dispersion of the produced velocities is affected also by this variable. From the analysis of the force signal, we assume for the holding force *F0* a Gaussian distribution with mean 0.3 N and standard deviation 0.05 N. This is likely to be a worst case assumption. If we consider that the experiment is repeated, the dispersion of the measured velocity (i.e., the differences between pairs of measured velocities) is given both by the dispersion of the applied preload *F0* and the dispersion of the behavior of adhesion:

$$\Delta v_{test} = \frac{\Delta F0}{\sqrt{m_{mockup} k_{needles}}} + \frac{1}{m_{mockup}} \Delta\left(\frac{\Delta U}{v_{RT}}\right) \tag{4}$$

Here the term $\Delta(\Delta U/v_{RT})$ is related to the difference of the behavior of adhesion at the same side between different tests, which is assumed descriptive of the difference of the behavior of adhesion between the two opposed sides. As a worst case, we assume that all the dispersion of the measured velocities is due to adhesion:

$$\Delta v_{test} \approx \frac{1}{m_{mockup}} \Delta\left(\frac{\Delta U}{v_{RT}}\right) \tag{5}$$

Therefore we can calculate:

$$\Delta\left(\frac{\Delta U}{v_{RT}}\right) = m_{mockup} \Delta v_{test} \tag{6}$$

By substituting Equation 6 into Equation 2 we get:

$$v_{flight} = \frac{1}{2} \frac{F0}{m_{TM}} \Delta t + \frac{m_{mockup}}{m_{TM}} \Delta v_{test} \tag{7}$$

Basically, the differences between pairs of measured velocities may be rescaled by the mass ratio and added to the velocity produced by the pushing forces.

Test Results

During every test, three signals are acquired: TM x-displacement, pitch and yaw angles (Figure 12). At the release, after a quick acceleration phase the TM mock-up moves with almost constant linear and angular (both pitch and yaw) velocities. Angular components of velocity are associated to misalignments of the release tip and the resultant of the forces applied by the three blocking needles with respect to the TM center of mass. However, the amount of kinetic energy due to angular velocities (pitch and yaw) after the release is negligible (0.5%) compared to that associated to the linear velocity. In Figure 13, the TM displacement and linear velocity are shown. The velocity signal is obtained as the discrete time derivative of the sampled displacement, and it is used to estimate the release time interval, after which the velocity can be considered constant. The final velocity is therefore estimated as the slope of the displacement

signal after the release, through a linear least square fit. Fit uncertainty is very small compared to the estimated final velocity.

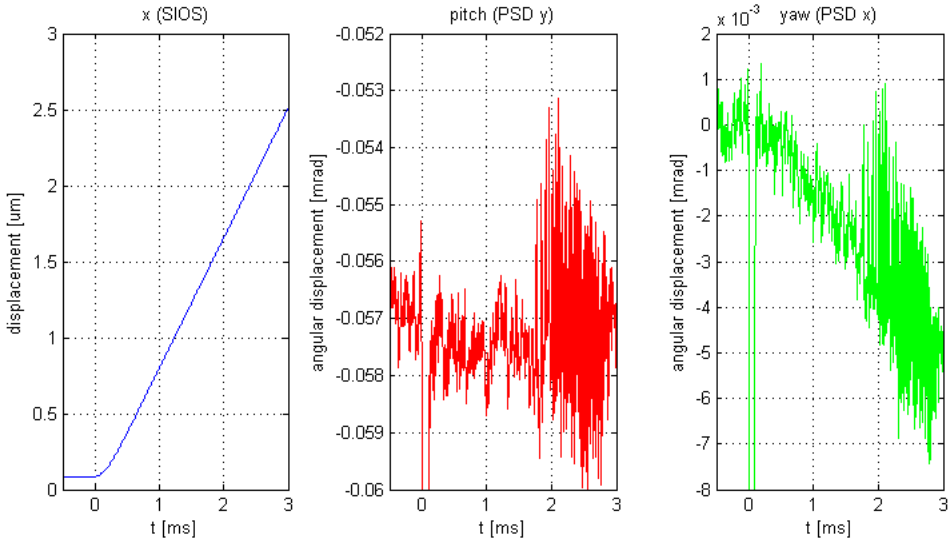

Figure 12. TM displacement, pitch and yaw signals

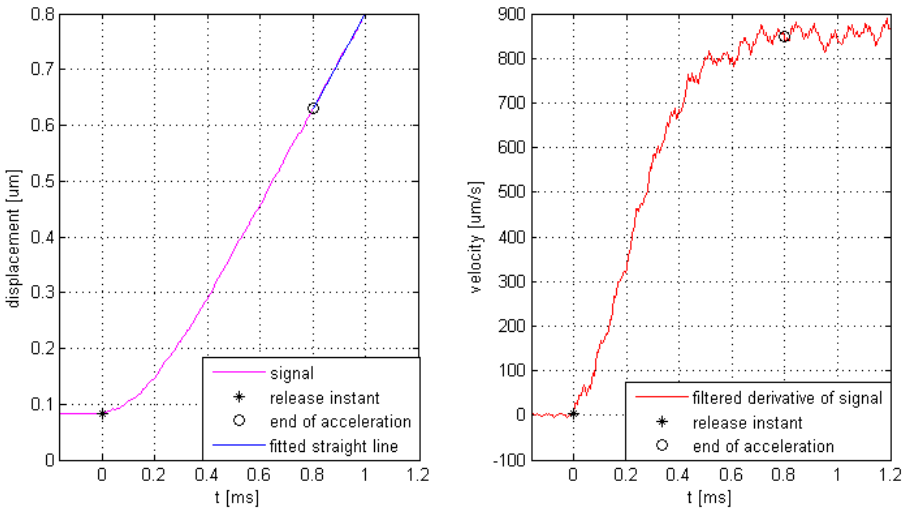

Figure 13. Example of TM displacement and velocity signal during the release phase, along (0°,0°) direction

The tests have been performed starting from the nominally aligned direction, searching the maximum release velocity. Across the measured maximum, a release tip misalignment of ±1.6 mrad (±0.092°) has been explored along both yaw and pitch directions. Ten repetitions have been done along each direction, and test of hypothesis has been performed to check the significance of the difference between the mean of a direction and its neighbors. Two directions are assumed to produce the same mean velocity when the p-value of the test of hypothesis is larger than 50%.

Table 1 shows the 10 measured velocities and their mean value for a single direction. The uncertainty of every estimated velocity is significantly smaller compared to the standard deviation of the direction, confirming that the measurement precision is adequate [15]. The results of the overall test campaign are

reported in Table 2. According to the literature [16][17], a direction of retraction of the tip which is misaligned with respect to the local orthogonal to the surface produces a shear stress which reduces adhesion force. As a consequence, a reduction of the release velocity is expected along the directions of retraction which are locally misaligned. The results show that the peak velocity is reached along two directions, namely (-0.3°, 0°) and (-0.3°,-0.092°). The velocities along the surrounding directions are significantly smaller, such that the hypothesis test rejects the hypothesis of equal mean values. Some of these directions produce velocities that are statistically consistent. The overall behavior of the release velocity is fairly regular and shows just an absolute maximum. Since the absolute maximum is reached along two directions, we assume that the worst-case misalignment of the release tip direction spans of ±1.6 mrad (±0.092°) around each, covering the yaw interval between -0.392° and -0.208° and pitch interval between -0.184° and +0.092°. This set of directions covers 120 tests, i.e., 120 values of the release velocity v_{test} of Equation 3. The distribution of the rescaled (i.e., multiplied by the mass ratio) velocities is plotted in Figure 14: the mean is 37.7 μm/s and the standard deviation is 1.5 μm/s.

Table 1. Estimated final velocities for one release direction (-0.3°, +0.092°)

test	final velocity (μm/s)	fit uncertainty (μm/s)
1	828.14	0.73
2	863.33	0.79
3	886.09	0.84
4	841.69	0.74
5	790.82	0.61
6	862.65	0.69
7	884.84	0.79
8	878.80	0.80
9	842.54	0.72
10	876.14	0.81
mean standard deviation	855.50 30.13	

Table 2. Mean final velocity (μm/s) of release directions. Neighbor numbers in equal colors are statistically consistent. Numbers in gray color have been measured while searching the direction of maximum with a large step (0.3°)

	Yaw (°)					
Pitch (°)	-0.6	-0.392	-0.3	-0.208	0	+0.3
+0.3					772	
+0.092		848	856	839		
0	820	807	873	843	847	847
-0.092		837	874	847		
-0.184		839	838	859		
-0.3					808	

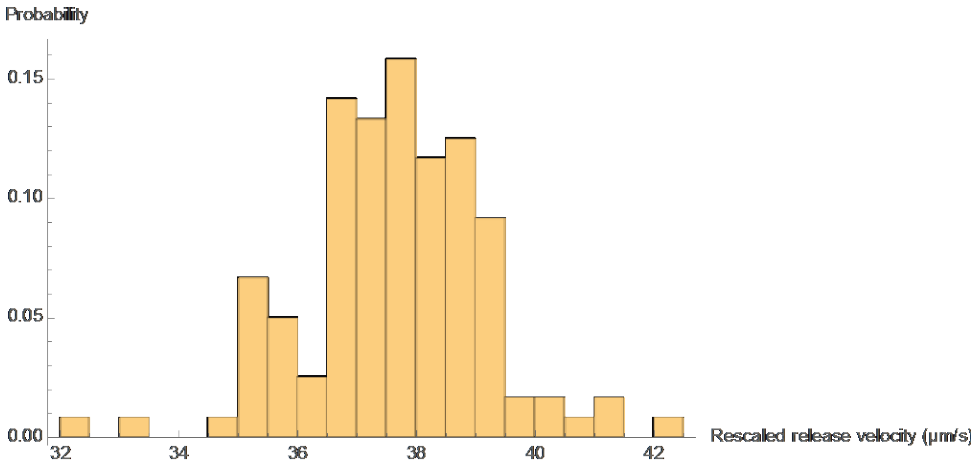

Figure 14. Rescaled v_{test} release velocities of 120 tests across the peak direction, covering yaw interval (-0.392°, -0.208°) and pitch interval (-0.184°, +0.092°)

The distribution of velocities plotted in Figure 14 is representative of an in-flight one-sided release and are heavily affected by the systematic push of the blocking needles. This contribution cancels out if the differences Δv_{test} between pairs of velocities is calculated. The statistical distribution of the rescaled Δv_{test} variable (second member of Equation 7) is plotted in Figure 15. The mean is zero (similarly to Figure 7) while the standard deviation is 2 µm/s.

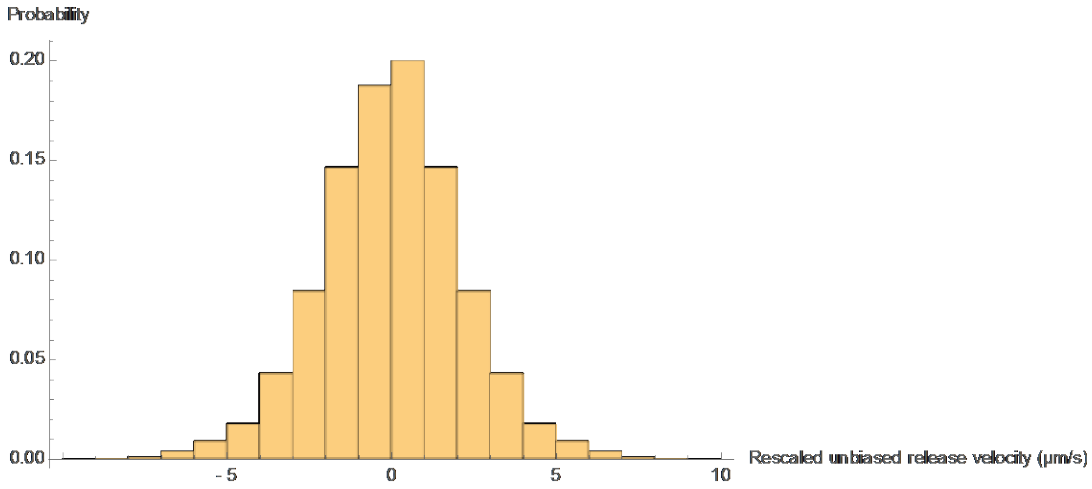

Figure 1. Rescaled Δv_{test} release velocities

Results synthesis

The results plotted in Figure 7 (effect of pushing forces) and Figure 15 (effect of adhesion) need to be convolved to obtain the resulting release velocity in flight, v_{flight} of Equation 7. The statistical distribution of the overall release velocity is shown in Figure 16. The mean is zero and the standard deviation is 2.2 µm/s. The probability of a compliant release (magnitude of v_{flight} less than 5 µm/s) is 96%. This result is compatible with the previous estimations of the release velocity [18] [19].

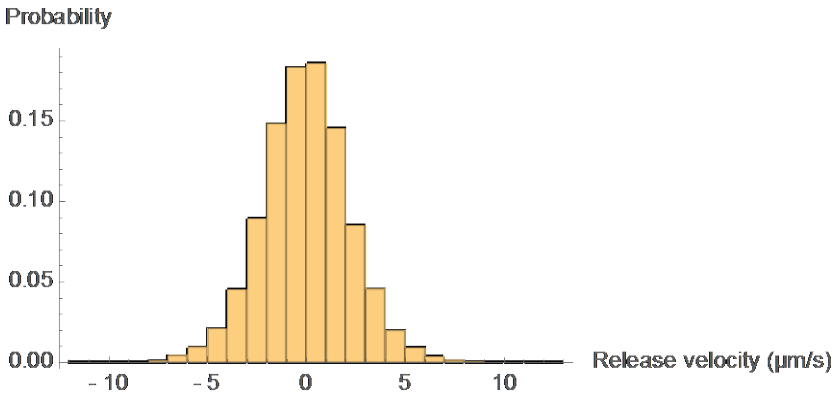

Figure 16. Overall release velocity in flight

Conclusions

The injection of an object into a geodesic trajectory constitutes a relevant space engineering challenge. In this paper we present a ground-based testing approach, which allowed us to provide the qualification of the mechanism designed and developed to perform the injection of a 2-kg gold-coated test mass into a geodesic trajectory of unprecedented purity (LISA Pathfinder). The criticality of the mechanism for its test mass injection into geodesic function mainly relies on the possible asymmetry of the two opposed actions on the test mass. Both the holding forces and following adhesive interaction between the test mass and its holding tips may produce a net impulse at the release, i.e., an excessive test mass residual velocity, when the dynamic behavior of the two opposed contact on the test mass results asymmetric.

The testing method and the test results for the Grabbing Positioning and Release Mechanism developed for the LISA Pathfinder mission are here presented and discussed.

References

1. F. Antonucci, et al. “The LISA pathfinder mission”. Classical Quantum Gravity, vol. 29, no. 12, pp. 124014-1–124014-11, 2012.
2. M. Armano et al. "The LISA Pathfinder Mission". Journal of Physics: Conference Series Volume 610, Issue 1, 11 May 2015, Article number 012005.
3. B. Zahnd, M. M. Zimmermann, and R. Spörri. “LISA-Pathfinder cage and vent mechanism — Development and qualification”. Proceedings of the 15th European Space Mechanisms and Tribology Symposium, 2013, pp. 1–7.
4. A. Neukom, R. Romano, and P. M. Nellen. “Testing and lesson learnt of LISA GPRM”. Proceedings of the 13th European Space Mechanisms and Tribology Symposium, 2009, pp. 1–8.
5. I. Köker, H. Rozemeijer, F. Stary, and K. Reichenberger. “Alignment and testing of the GPRM as part of the LTP caging mechanism”. Proceedings of the 15th European Space Mechanisms and Tribology Symposium, 2013, pp. 1–7.
6. M. Benedetti, D. Bortoluzzi, M. D. Lio, and V. Fontanari. “The influence of adhesion and sub-Newton pull-off forces on the release of objects in outer space”. J. Tribology, vol. 128, no. 4, pp. 828–840, 2006.
7. D. Bortoluzzi, M. De Cecco, S. Vitale, and M. Benedetti. “Dynamic measurements of impulses generated by the separation of adhered bodies under near-zero gravity conditions”. Exp. Mech., vol. 48, pp. 777–787, 2008.
8. D. Bortoluzzi, M. Benedetti, L. Baglivo, and S. Vitale. “A new perspective in adhesion science and technology: Testing dynamic failure of adhesive junctions for space applications”. Exp. Mech., vol. 50, pp. 1213–1223, 2010.

9. D. Bortoluzzi, M. Benedetti, and J. W. Conklin. “Indirect measurement of metallic adhesion force as a function of elongation under dynamic conditions”. Mech. Syst. Signal Process, vol. 38, no. 2, pp. 384–398, 2013.
10. D. Bortoluzzi, L. Baglivo, M. Benedetti, F. Biral, P. Bosetti, A. Cavalleri, M. D. Lio, M. D. Cecco, R. Dolesi, M. Lapolla, W. Weber, and S. Vitale. “Lisa pathfinder test mass injection in geodesic motion: status of the on ground testing”. Classical Quantum Gravity, vol. 26, no. 9, pp. 094011-1–094011-11, 2009.
11. C. Zanoni, D. Bortoluzzi, J. Conklin, I. Köker, C.Marirrodriga, P. Nellen, and S. Vitale. “Testing the injection of the LISA-pathfinder test mass into geodesic conditions”. Proceedings of the 15th European Space Mechanisms and Tribology Symposium, 2013, pp. 1–10.
12. D. Bortoluzzi, M. Benedetti, L. Baglivo, M. De Cecco, S. Vitale. “Measurement of momentum transfer due to adhesive forces: On-ground testing of in-space body injection into geodesic motion”. Rev. Sci. Instrum. 82, 125107 (2011).
13. D. Bortoluzzi, P. A. Mäusli, R. Antonello, and P. M. Nellen. “Modeling and identification of an electro-mechanical system: The LISA grabbing positioning and release mechanism case”. Adv. Space Res., vol. 47, no. 3, pp. 453–465, 2011.
14. M. Benedetti, D. Bortoluzzi, and S. Vitale. “A momentum transfer measurement technique between contacting free-falling bodies in the presence of adhesion”. J. Appl. Mech., vol. 75, no. 1, p. 011016, 2008.
15. M. D. Cecco, D. Bortoluzzi, L. Baglivo, M. Benedetti, and M. D. Lio. “Measurement of the momentum transferred between contacting bodies during the Lisa test-mass release phase uncertainty estimation”. Meas. Sci. Technol., vol. 20, no. 5, pp. 055101-1–055101-15, 2009.
16. K. Rabenorosoa, C. Clévy, P. Lutz, M. Gauthier, P. Rougeot, Micro & Nano Letters, 2009, Vol. 4, Iss. 3, pp. 148–154.
17. A. R. Savkoor and G. A. D. Briggs , Proceedings of the Royal Society of London. Series A, Mathematical and Physical Sciences, Vol. 356, No. 1684 (Aug. 15, 1977), pp. 103-114.
18. D. Bortoluzzi, J. W. Conklin, and C. Zanoni. “Prediction of the LISA Pathfinder release mechanism in-flight performance”. Adv. Space Res., vol. 51, no. 7, pp. 1145–1156, 2013.
19. C. Zanoni and D. Bortoluzzi. "Experimental-Analytical Qualification of a Piezoelectric Mechanism for a Critical Space Application". IEEE/ASME Transactions on Mechatronics, Vol. 20, No. 1, February 2015.